Ubiquitous Nonlocal Entanglement with Majorana Zero Modes

Alessandro Romito[1] and Yuval Gefen[2]
[1]Department of Condensed Matter Physics, The Weizmann Institute of Science, Rehovot 76100, Israel
[2]Department of Physics, Lancaster University, Lancaster LA1 4YB, United Kingdom
(Received 29 March 2017; published 13 October 2017)

Entanglement in quantum mechanics contradicts local realism and is a manifestation of quantum nonlocality. Its presence can be detected through the violation of Bell, or Clauser-Horne-Shimony-Holt (CHSH) inequalities. Paradigmatic quantum systems provide examples of both, nonentangled and entangled states. Here, we consider a minimal complexity setup consisting of six Majorana zero modes. We find that any allowed state in the degenerate Majorana space is nonlocally entangled. We show how to measure (with available techniques) the CHSH-violating correlations using either intermediate strength or weak measurement protocols.

DOI: 10.1103/PhysRevLett.119.157702

Introduction.—Majorana zero modes are particular non-Abelian quasiparticles that reflect the topologically nontrivial character of the underlying system. Over less than a decade, Majorana zero modes (MZM) have crossed the line from mathematically intriguing solid state manifestations of Majorana's original particles [1–3], to experimentally realizable entities [4–6]. Being a class of non-Abelian anyons [7,8], MZM offer a paradigm for fault-tolerant information processing [9]. Following initial experiments [10–15], we are now at the stage where specific platforms for engineering and manipulating Majoranas [16–18] are being implemented. It is broadly felt that implementations of topological states of matter for quantum information processing should rely, first, on a thorough understanding of quantum states defined by Majorana zero modes. Interestingly, a unique property of MZM is that they may constitute a manifestation of quantum nonlocality. Indirect observable signatures emerging from nonlocal MZM (albeit not a proof of their nonlocality) have been studied earlier in setups based on mesoscopic superconductors [19–21] or coupled Majorana zero modes [22,23].

Nonlocality is an indispensable pillar of quantum mechanics. For a system made of at least two particles, nonlocality is a manifestation of quantum entanglement between spatially distinct degrees of freedom. For paradigmatic systems, an apt example being two spin-1/2 particles, it is possible to construct both entangled (e.g., a singlet) and nonentangled, i.e., product (e.g., triplet-1) states [24]. Quantum nonlocality is quantified by Bell's inequality [25], or, in a manner that is more conducive to experimental testing [26,27], by the violation of the Clauser-Horne-Shimony-Holt (CHSH) inequality [28]. Entanglement properties of Majorana systems have been explored as a source of nonlocality [29] for applications to certifiable random numbers generation [30] and for extending protected operations beyond braiding [31].

The focus of the present Letter is the direct observability of distinct entanglement features of quantum states in the degenerate space defined by Majorana zero modes. We identify a system of minimal complexity (minimal number of MZM). For that system, (i) we show that any allowed quantum state in the degenerate space defined by a set of MZM is nonlocally entangled, (ii) we then demonstrate how such entanglement can be detected within technologically feasible measurement platforms, and finally, (iii) we show how our entanglement detection protocol can be realized within weak measurement operations.

Model.—Our system consists of a multiterminal junction made up of an even number of one-dimensional topological superconductors (branches) depicted in Fig. 1(a). They all have a common end point at the center. Such junctions can be engineered experimentally with semiconductor wires [10–12,14] or magnetic impurity chains [13]. Each segment, $\alpha \in \{1, \ldots, 2N\}$, of this setup consists of a 1D spinless p-wave superconductor characterized by a bulk excitation energy gap, Δ_α, and by zero-energy MZM at the end points, γ_α, γ'_α, localized at the wire's boundaries. The dynamics of these MZM is underlined by the algebra $\{\gamma_\alpha, \gamma_\beta\} = 2\delta_{\alpha,\beta}$, $\{\gamma_\alpha, \gamma'_\beta\} = 0$. The wire Hamiltonian at energies well below the gap is given by $H_\alpha = \epsilon_\alpha \gamma_\alpha \gamma'_\alpha$, where $\epsilon_\alpha \sim e^{-l_\alpha/\xi_\alpha}$ is exponentially small with the wire's length, l_α. The latter is larger than the superconductor coherence length [3–5] $\xi_\alpha \propto 1/\Delta_\alpha$. We also assume $\epsilon_\alpha = 0$, which is a valid assumption as long as the duration of the measurement protocol is not too long. At the junction, the Josephson coupling between each pair of branches, α, β results in a low energy coupling between the corresponding Majorana end states. This is described by the tunneling Hamiltonian [3,32] $H_T = \sum_{\alpha,\beta} t_{\alpha,\beta} \gamma'_\alpha \gamma'_\beta$, which, generically, pairs up the $2N$ Majorana zero modes, $\gamma'_1, \ldots, \gamma'_{2N}$, to finite energy states with energies $\sim \min\{t_{\alpha,\beta}\}$. These states are then projected out of the degenerate ground-state space. The MZM $\{\gamma_\alpha\}$ far from the junction [see Fig. 1(a)] represent the remaining zero energy degrees of freedom, which span a 2^N degenerate ground state. The Majorana

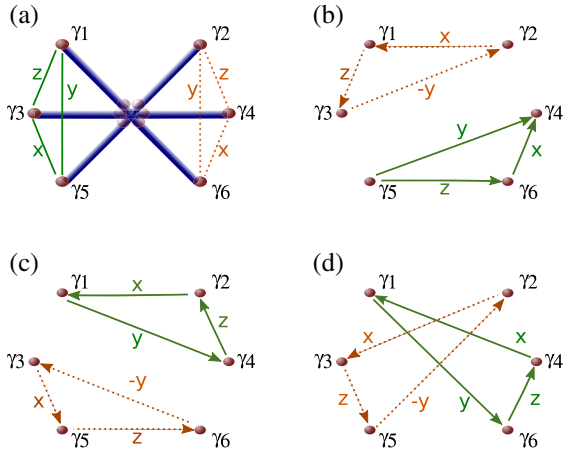

FIG. 1. (a) Multiterminal junction of topological superconducting wires (blue) hosting Majorana zero modes at their ends (red dots). The Majorna end-states at the junction (fading red) are gapped up and the six Majorana end states (solid red dots) $\gamma_1, \ldots, \gamma_6$ constitute the low energy excitations of the system. A left detector (not shown) measures the operators indicated by solid (green) arrows, which are labeled by the corresponding spin algebra operators, e.g., $Z = -i\gamma_1\gamma_2$ playing the role of σ_z. Dashed (orange) arrows define the operators measured by the right detector. Panels (a)–(d) show different possible partitionings into left and right sectors with the corresponding operators. CHSH inequalities are necessarily violated in at least one of the partitionings in (a)–(d).

subspace does not accommodate a well-defined number of fermions: it may exchange pairs of fermions with the underlying superconductor. It follows that the parity of the Majorana system, $\mathcal{P} = i\prod_{j=1}^{2N}\gamma_j$, is a good quantum number; hence, the degenerate ground-state space consists of two subspaces, each of a definite parity. Without loss of generality, we may restrict ourselves, in the low-energy space, to states in the 2^{N-1}-dimensional odd subspace. We will study a minimal complexity setup consisting of $2N = 6$ MZM.

The MZM, $\gamma_1, \ldots, \gamma_{2N}$, can be partitioned into two different sets, left (L) and right (R), each of which is to be probed by a separate external detector. The detectors can be tuned to measure any combination of pairs of Majorana products. Physically, this is a measurement of the occupancy of certain Dirac fermions degrees of freedom, constructed from the Majorana degrees of freedom. Details of the measurement procedure are discussed below. An example to be utilized below is depicted in Fig. 1(a), where the L set consists of γ_1, γ_3, γ_5, and the coupled detector can measure any operator of the form

$$\hat{O}_L = -i(\cos\theta_L\gamma_1\gamma_3 + \sin\theta_L\cos\phi_L\gamma_3\gamma_5 + \sin\theta_L\sin\phi_L\gamma_5\gamma_1). \quad (1)$$

Note that the expectation values of the measured observables are bounded, $-1 \le \langle O_L\rangle \le 1$ (the eigenvalues of the bilinear Majorana products are ± 1). Genuine quantum correlations underlying a state can be identified through the expectation values of correlated measurements. Specifically, a state that can be described within a local hidden variable theory (also known as local realism), satisfies the CHSH inequality [28]

$$\mathcal{C} \equiv |\langle \hat{O}_L\hat{O}_R\rangle - \langle \hat{O}_L\hat{O}'_R\rangle| + |\langle \hat{O}'_L\hat{O}'_R\rangle + \langle \hat{O}'_L\hat{O}_R\rangle| \le 2, \quad (2)$$

where $\hat{O}_L$, $\hat{O}'_L$ and $\hat{O}_R$, $\hat{O}'_R$ are pairs of spatially separable sets of observables. Instead, for quantum nonlocally entangled states, it is possible to choose the operators such that [33] $2 < \mathcal{C} \le 2\sqrt{2}$, hence, providing evidence of genuine quantum correlations. Equation (2) is an equivalent formulation of Bell's inequality [25,28], which, relying only on averaged correlation outputs, can be tested directly by averaging over repeated measurements, including weak measurements.

A quantum system generically realizes both entangled states that violate Bell's (hence, CHSH) inequalities and product states. The novel aspect of our work is that we show that, in the degenerate space spanned by Majorana zero modes, any state is nonlocally entangled. In other words, one can always find (at least) one partitioning of the MZM into two spatially separable sets, where the CHSH inequality is violated. Loosely speaking, for any state in the degenerate ground space, it is possible to design nonlocal measurements that reveal intrinsic nonlocality.

To begin with, we realize that establishing the CHSH relations requires the measurement of noncommuting observables for each of the separated-in-space parts of the system, i.e., the L and R sets. For observables bilinear in the elementary MZM [cf. Eq. (1)], this requires a minimum of three Majorana operators for each set. Therefore, the minimal complexity setup appropriate for our purpose is a multiterminal junction consisting of six branches (six MZM) [cf. Fig. 1(a)]. We consider a generic state of the four-degenerate odd parity ground manifold. Following the labeling of the Majoranas in Fig. 1(a), such a state is parametrized as

$$|\psi\rangle = Ad^\dagger_{1,3}d^\dagger_{4,2}d^\dagger_{5,6}|0\rangle + Bd^\dagger_{1,3}|0\rangle + Cd^\dagger_{4,2}|0\rangle - Dd^\dagger_{5,6}|0\rangle, \quad (3)$$

where $|A|^2+|B|^2+|C|^2+|D|^2=1$. Here, we have introduced the fermionic degrees of freedom, $d^\dagger_{1,3}=(\gamma_1+i\gamma_3)/2$ $d^\dagger_{4,2} = (\gamma_4 + i\gamma_2)/2$, $d^\dagger_{5,6}=(\gamma_5+i\gamma_6)/2$, and the state $|0\rangle$ is defined by $d_{1,3}|0\rangle=0$, $d_{5,6}|0\rangle=0$, $d_{4,2}|0\rangle=0$. Throughout our analysis, we will switch between Fock space states, spin-1/2 states, and Majorana notation.

Consider the partitioning depicted in Fig. 1(a): γ_1, γ_3, γ_5 constitute the (L) set; γ_2, γ_4, γ_6, the (R) set. The operators $\hat{Z}_L \equiv -i\gamma_1\gamma_3$, $\hat{X}_L \equiv -i\gamma_3\gamma_5$, and $\hat{Y}_L \equiv -i\gamma_5\gamma_1$ satisfy the Pauli matrix algebra, $\sigma_z = \hat{Z}_L$, $\sigma_x = \hat{X}_L$, and $\sigma_y = \hat{Y}_L$. It follows that the measurement of an operator of the form of

Eq. (1) can be mapped onto the measurement of $\hat{O}_L = \hat{\boldsymbol{\sigma}} \cdot \mathbf{n}$, where $\hat{\boldsymbol{\sigma}} = 2\hat{\mathbf{S}}$ is a spin-1/2 operator and $\mathbf{n} \equiv (\sin\theta_L \cos\phi_L, \sin\theta_L \sin\phi_L, \cos\theta_L)$. Analogously, $\hat{Z}_R \equiv -i\gamma_4\gamma_2$, $\hat{Y}_R \equiv i\gamma_2\gamma_6$, and $\hat{X}_R \equiv -i\gamma_6\gamma_4$ can be identified with Pauli operators of the right set. In such spin-1/2 language, the state $|\psi\rangle$ reads $|\psi\rangle = A|\uparrow_L\uparrow_R\rangle + B|\uparrow_L\downarrow_R\rangle + C|\downarrow_L\uparrow_R\rangle + D|\downarrow_L\downarrow_R\rangle$, where $|\uparrow_i\rangle$ $|\downarrow_i\rangle$ are the eigenstates of $\hat{Z}_i$ ($i = L, R$). The maximal value of the CHSH correlation $\mathcal{C}$ in Eq. (2) is given by

$$\mathcal{C}_{135|246} = 2\sqrt{1 + 4|AD - BC|^2}, \tag{4}$$

where the subscript indicates the partitioning in which the measurement is performed. For any state, $2 \leq \mathcal{C}_{135|246} \leq 2\sqrt{2}$, and $\mathcal{C}_{135|246} \neq 2$ signals nonlocal correlations, which happens unless $AD - BC = 0$. Operationally, this means that, if $AD - BC \neq 0$ one can select the coefficients θ_L, θ_R, ϕ_L, ϕ_R to construct a proper set of operators that violate the CHSH inequality.

Though a given state might not violate the CHSH inequality with measurements within the specific L and R sets, it can still lead to a violation of the CHSH inequality with a different partitioning of the MZM. The new partitioning will be nonlocal in the old L and R sets. For example, a different partitioning consisting of the sets $\tilde{L}$ and $\tilde{R}$ is depicted in Fig. 1(b), where the left detector is connected to γ_5, γ_6, γ_4 while γ_1, γ_3, γ_2 are connected to the right detector. In this case, we define he operators $\hat{Z}_{\tilde{L}} \equiv -i\gamma_5\gamma_6$, $\hat{X}_{\tilde{L}} \equiv -i\gamma_6\gamma_4$, $\hat{Y}_{\tilde{L}} \equiv -i\gamma_4\gamma_5$, and $\hat{Z}_{\tilde{R}} \equiv -i\gamma_1\gamma_3$, $\hat{Y}_{\tilde{L}} \equiv i\gamma_3\gamma_2$, $\hat{X}_{\tilde{L}} \equiv -i\gamma_2\gamma_1$. Mapping the problem to that of a two spin-1/2 system, we can write the state $|\psi\rangle$ in Eq. (3) as $|\psi\rangle = \tilde{A}|\tilde{\uparrow}_L\tilde{\uparrow}_R\rangle + \tilde{B}|\tilde{\uparrow}_L\tilde{\downarrow}_R\rangle + \tilde{C}|\tilde{\downarrow}_L\tilde{\uparrow}_R\rangle + \tilde{D}|\tilde{\downarrow}_L\tilde{\downarrow}_R\rangle$, where $\tilde{A} = A$, $\tilde{B} = D$, $\tilde{C} = B$, $\tilde{D} = C$, and $|\tilde{\uparrow}_i\rangle$, $|\tilde{\downarrow}_i\rangle$ are the eigenstates of $\tilde{Z}_i$. For the given A, B, C, D, the maximal violation of the CHSH inequalities in the new partitioning [maximal with respect of the choice of $\hat{O}_L$, $\hat{O}_R$, cf. Eq. (1)] is given by

$$\mathcal{C}_{564|132} = 2\sqrt{1 + 4|AC - DB|^2}, \tag{5}$$

where $\mathcal{C}_{135|246} > 2$ signals nonlocal correlations. This is achieved unless $AC - BD = 0$. Measurements of CHSH inequalities following the partitionings depicted in panels (c) and (d) of Fig. 1 yield $\mathcal{C}_{421|563} = 2\sqrt{1 + 4|AB - CD|^2}$ and $\mathcal{C}_{641|352} = 2\sqrt{1 + |A^2 + C^2 + D^2 - B^2|^2}$. The condition $\mathcal{C}_{135|246} = \mathcal{C}_{136|245} = \mathcal{C}_{456|123} = \mathcal{C}_{124|356} = 2$ can never be satisfied; i.e., CHSH correlations will be nonlocal in at least one of the four partitions considered in Fig. 1.

It is important, at this point, to make the following observation. The partitioning of the MZM into two sets naturally leads to the definition of operators satisfying spin-1/2 algebra for each set. Different partitionings entail different sets of spin operators. Such a construction of operators is not unique for MZM. It can be done for any quantum system whose state is spanned in a four-dimensional space. Consider the case of two real, physical, spin-1/2 degrees of freedom, associated with L and R, respectively, which are geographically separated. One may construct the corresponding sets of operators Z_i, X_i, Y_i, as is depicted in Fig. 1(a). Now, we would like to switch to another partitioning [e.g., the one depicted in Fig. 1(b)], involving $\tilde{R}$ and $\tilde{L}$, respectively. Trying to express the spin operators associated with this partitioning in terms of the real spin operators, we have $\hat{Z}_{\tilde{R}} = \hat{Z}_L$, and $\hat{Z}_{\tilde{L}} = \hat{Z}_L \otimes \hat{Z}_R$. It follows, then, that $Z_{\tilde{R}}$ and $Z_{\tilde{L}}$ cannot be measured by two spatially separated detectors. This is in stark contrast with the foregoing Majorana-based picture.

The statement that any state of the system violates the CHSH inequalities in at least one of the partitionings of Fig. 1 implies finite violation of CHSH inequalities. This is quantified by introducing the maximal value of CHSH correlations over the partitioning in Fig. 1, $\mathcal{C}_0(|\psi\rangle) \equiv \max\{\mathcal{C}_{135|246}, \mathcal{C}_{564|132}, \mathcal{C}_{421|563}, \mathcal{C}_{641|352}\}$. For any $|\psi\rangle$, $\mathcal{C}_0(|\psi\rangle) - 2$ is a positive finite quantity. Therefore, there is a minimum violation of the CHSH inequality over all states. From a standard minimization procedure over the parameters A, B, C, D [34], we obtain

$$\min_{|\psi\rangle}\{\mathcal{C}_0(|\psi\rangle)\} \approx 2.031. \tag{6}$$

Note that, since we restrict the analysis here to the four configurations of Fig. 1, the minimum value obtained is, in fact, a lower bound of the optimal minimum entanglement.

Measurement.—In order to implement the above ideas, we need to measure operators of the form (1) and correlations thereof. While the emerging picture is quite general, we will demonstrate it by resorting to a specific measurement protocol: weakly tunnel-coupling quantum dots (QDs) to the multiterminal Majorana junction [35,36], and then measuring their charge. Let us describe the measurement procedure for operators associated with the L and R Majorana sets. We correspondingly define L and R detectors, each consisting of a double quantum dot tunnel-coupled to the three MZM in the set, as shown in Fig. 2. The coupling of the L detector to the corresponding MZM is given by the Hamiltonian

$$\begin{aligned} H_{\mathrm{det,L}} = {} & w_{3,Q}\gamma_3(c_{Q,L} - c_{Q,L}^\dagger) + w_{3,P}\gamma_3(c_{P,L} - c_{P,L}^\dagger) \\ & + w_{1,Q}\gamma_1(c_{Q,L} - c_{Q,L}^\dagger) + w_{5,P}\gamma_5(c_{P,L} - c_{P,L}^\dagger), \end{aligned} \tag{7}$$

where $c_{j,L}$, $j = Q, P$ are the electron destruction operators of each dot of the pair (all electrons are spin polarized) and $w_{\alpha,j}$ are the tunneling matrix elements between the superconductor's end points and the quantum dots. These dots are tuned such that only one orbital level per dot is relevant at the energy scales considered. The charge configuration

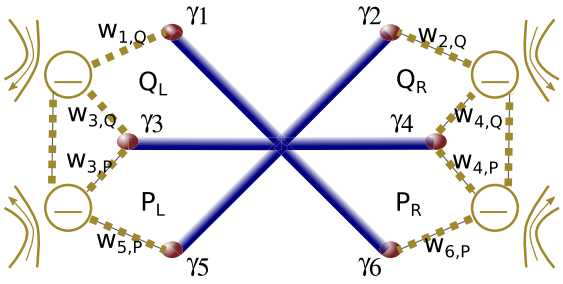

FIG. 2. Measurement of CHSH correlations in a multiterminal Majorana junction. The left and right measurement apparatus consist of quantum dots (Q_L, P_L, Q_R, P_R) properly coupled to the MZM via tunnel coupling (dotted lines) of strength $w_{\alpha,j}$. The charge configuration of each dot is detected by a nearby charge sensor, schematically depicted as a quantum point contact. The measurement is performed by controlled time pulsed activations of the tunnel coupling $w_{\alpha,j}$.

of the double QD, $(n_{Q,L}, n_{P,L})$, with $n_j = 0$, 1 can be detected by fast charge sensors, e.g., quantum point contacts [37–44]. The possibly time dependent tunnel coupling is controlled, e.g., by a nearby gate voltage [45]. One initially prepares the decoupled double QD in a generic superposition of singly occupied levels, $|\phi_0\rangle = p_L|0,1\rangle + q_L|1,0\rangle$, where $|p_L|^2 + |q_L|^2 = 1$. The tunnel coupling is then switched on for a finite time Δt and is, subsequently, switched off. The state of the QDs may be modified, and the new charge configuration is read out by the charge sensors. Specifically, we access the probability, $\mathcal{P}^L_{(1,0)}$, of finding the double dots in the configuration (1, 0).

While the strength and the duration of the QD-Majorana coupling is adjustable, we consider, here, for simplicity, the weak measurement limit. (Going beyond this limit is discussed below [34].) Expanding the time evolution, $U = e^{-iH_{\mathrm{det,L}}\Delta t}$, due to the system-detector coupling for small Δt, and setting, for simplicity, the initial state of the double QD to $p_L = -iq_L = -i/\sqrt{2}$ and $w_{\alpha,j} \in \mathbb{R}$, the measured probability reads $\mathcal{P}^L_{(1,0)} \approx 1/2 - (\eta_L - \lambda_L\langle\hat{O}_L\rangle)(\Delta t)^2$ to leading order in $\eta_L = (|w_{1,Q}|^2 + |w_{3,Q}|^2 + |w_{3,P}|^2 + |w_{5,P}|^2)/2$, $\lambda_L = [(w_{1,Q}w_{3,P})^2 + (w_{3,Q}w_{5,P})^2 + (w_{1,Q}w_{5,P})^2]^{1/2}$. Here, $\hat{O}_L$ takes the form of Eq. (1) with $\cos\theta_L = w_{1,Q}w_{3,P}/\lambda_L$, $\sin\theta_L \cos\phi_L = -w_{3,Q}w_{5,P}/\lambda_L$, $\sin\theta_L \sin\phi_L = w_{5,P}w_{1,Q}/\lambda_L$. For $\lambda_L(\Delta t)^2 \ll 1$ and $\eta_L(\Delta t)^2 \ll 1$, this procedure constitutes a weak measurement of the operator $\hat{O}_L$. Tuning the parameters $w_{i,j}$, $i = 1, 3, 5$ and $j = Q, P$ covers all operators of the local algebra of the left (L) set. The same may be repeated to measure the observables represented by the operators $\hat{O}_R$ of the right set, and the correlated measurements implied by the CHSH inequality are, therefore, executable. Specifically, referring to Fig. 2, one begins with the configuration $p_L = p_R = -iq_L = -iq_R = -i/\sqrt{2}$. Tunnel coupling the MZM to the QDs, and then sensing their final configuration, the probability to end up in the $(n_{Q,L} = 1, n_{P,L} = 0, n_{Q,L} = 1, n_{Q,R} = 0)$ is

$$\mathcal{P}_{(1,0,1,0)} = \mathcal{P}^L_{(1,0)}\mathcal{P}^R_{(1,0)} + \frac{(\Delta t)^4}{6}(\eta_L^2 + \eta_R^2 + \lambda_L^2 + \lambda_R^2 + 2\eta_L\lambda_L\langle\hat{O}_L\rangle + 2\eta_R\lambda_R\langle\hat{O}_R\rangle + \lambda_L\lambda_R\langle\hat{O}_L\hat{O}_R\rangle), \tag{8}$$

where $\lambda_R = (w_{2,Q}w_{6,P})^2 + (w_{2,Q}w_{4,P})^2 + (w_{4,Q}w_{6,P})^2$ and $\eta_R = (|w_{2,Q}|^2 + |w_{4,Q}|^2 + |w_{4,P}|^2 + |w_{6,P}|^2)/2$. Equation (8) provides us with a way to evaluate the correlators of the type $\langle\hat{O}_L\hat{O}_R\rangle$ [cf. Eq. (2)]. To demonstrate how entanglement (violation of CHSH) is detected concretely in our measurement scheme, consider, specifically, the case of a state in Eq. (3) prepared with $A = D = 0$. The state is maximally entangled in the configuration of Fig. 1(a), and the operators $\hat{O}_L$, $\hat{O}'_L$, $\hat{O}_R$, and $\hat{O}'_R$ required for the maximal violation of the CHSH inequality [34,46] are obtained in our scheme by tuning $w_{5,P} = 0$, $w_{1,Q} = 0$, $w_{2,Q} = -w_{6,P} \ll w_{4,Q} = w_{4,P}$, and $w_{2,Q} = w_{6,P} \ll w_{4,Q} = w_{4,P}$, respectively. The same state, CHSH-tested with the configuration of Fig. 1(b), leads to no violation of the CHSH inequalities.

A few aspects of the measurement procedure are noteworthy. First, since the operators of the left and of the right sets commute, they can be measured simultaneously; nonuniversal details of the time sequence concerning on-and-off switching of the tunneling matrix elements are immaterial. Second, the weak limit of the measurement offers a simple interpretation of the results; however, the essence of the analysis remains unchanged at stronger system-detector interaction, although the calibration of the detector may become more involved. Finally, the proposed measurement protocol requires control of the individual tunnel matrix elements between the dots and the wires in order to measure different operators. This might present an experimental challenge. The required protocol operations may be realized by variants better suited to experimental implementation, e.g., by controlling individual QD's energy levels, or possibly by Majorana-to-charge conversion measurements [16].

Conclusions.—We have identified a minimal complexity MZM array, a junction with six segments delineating an eightfold degenerate subspace defined by six Majorana zero modes. Unlike paradigmatic quantum states of two spin-1/2 particles that may (e.g., spin singlet) or may not (spin triplet-1) be entangled, we have shown that any state in the four-dimensional fixed-parity degenerate space (e.g., odd parity) is nonlocally entangled. This comes with a minimal bound on the violation of the CHSH inequality [Eq. (6)]. We also presented a detector design based on MZM-QD tunnel coupling, amenable to experimental implementation, and showed how to obtain CHSH correlation functions. Specifically, we discussed the limit of a weak measurement protocol. This ubiquitous nonlocality,

expressed through nonlocal entanglement, reflects the intrinsic property of MZM as carriers of a fractionalized fermionic degree of freedom. Verification of nonlocal entanglement requires repeated measurements of CHSH correlations on replicas of the same state, with at least four different partitionings (into L and R sets) of the Majorana degrees of freedom. The CHSH inequality will be broken for at least one of these partitionings.

We acknowledge support from Israel Science Foundation, Grant No. 1349/14, Deutsche Forschungsgemeinschaft, Grant No. RO 2247/8-1, Collaborative Research Center 183 of the DFG, the Israeli Ministry of Science Israel-Russia program, and the Minerva Foundation.

[1] G. Moore and N. Read, Nucl. Phys. **B360**, 362 (1991).
[2] N. Read and D. Green, Phys. Rev. B **61**, 10267 (2000).
[3] A. Kitaev, Phys. Usp. **44**, 131 (2001).
[4] R. M. Lutchyn, J. D. Sau, and S. Das Sarma, Phys. Rev. Lett. **105**, 077001 (2010).
[5] Y. Oreg, G. Refael, and F. von Oppen, Phys. Rev. Lett. **105**, 177002 (2010).
[6] F. Wilczek, Nat. Phys. **5**, 614 (2009).
[7] F. Wilczek, Phys. Rev. Lett. **49**, 957 (1982).
[8] A. Stern, Nature (London) **464**, 187 (2010).
[9] C. Nayak, S. H. Simon, A. Stern, M. Freedman, and S. Das Sarma, Rev. Mod. Phys. **80**, 1083 (2008).
[10] V. Mourik, K. Zuo, S. M. Frolov, S. R. Plissard, E. P. A. M. Bakkers, and L. P. Kouwenhoven, Science **336**, 1003 (2012).
[11] A. Das, Y. Ronen, Y. Most, Y. Oreg, M. Heiblum, and H. Shtrikman, Nat. Phys. **8**, 887 (2012).
[12] H. O. H. Churchill, V. Fatemi, K. Grove-Rasmussen, M. T. Deng, P. Caroff, H. Q. Xu, and C. M. Marcus, Phys. Rev. B **87**, 241401 (2013).
[13] S. Nadj-Perge, I. K. Drozdov, J. Li, H. Chen, S. Jeon, J. Seo, A. H. MacDonald, B. A. Bernevig, and A. Yazdani, Science **346**, 602 (2014).
[14] S. M. Albrecht, A. P. Higginbotham, M. Madsen, F. Kuemmeth, T. S. Jespersen, J. Nygård, P. Krogstrup, and C. M. Marcus, Nature (London) **531**, 206 (2016).
[15] M. T. Deng, S. Vaitiekènas, E. B. Hansen, J. Danon, M. Leijnse, K. Flensberg, J. Nygard, P. Krogstrup, and C. M. Marcus, Science **354**, 1557 (2016).
[16] D. Aasen, M. Hell, R. V. Mishmash, A. Higginbotham, J. Danon, M. Leijnse, T. S. Jespersen, J. A. Folk, C. M. Marcus, K. Flensberg *et al.*, Phys. Rev. X **6**, 031016 (2016).
[17] S. Plugge, L. A. Landau, E. Sela, A. Altland, K. Flensberg, and R. Egger, Phys. Rev. B **94**, 174514 (2016).
[18] S. Plugge, A. Rasmussen, R. Egger, and K. Flensberg, New J. Phys. **19**, 012001 (2017).
[19] L. Fu, Phys. Rev. Lett. **104**, 056402 (2010).
[20] K. Michaeli, L. A. Landau, E. Sela, and L. Fu, arXiv:1608.00581.
[21] S. Vijay and L. Fu, Phys. Rev. B **94**, 235446 (2016).
[22] B. Zocher and B. Rosenow, Phys. Rev. Lett. **111**, 036802 (2013).
[23] S. Rubbert and A. R. Akhmerov, Phys. Rev. B **94**, 115430 (2016).
[24] Hereafter, we refer to entanglement of spatially distinct degrees of freedom.
[25] J. Bell, Physics **1**, 195 (1965).
[26] M. Giustina, M. A. M. Versteegh, S. Wengerowsky, J. Handsteiner, A. Hochrainer, K. Phelan, F. Steinlechner, J. Kofler, J.-Å. Larsson, C. Abellán *et al.*, Phys. Rev. Lett. **115**, 250401 (2015).
[27] B. Hensen, H. Bernien, A. E. Dréau, A. Reiserer, N. Kalb, M. S. Blok, J. Ruitenberg, R. F. L. Vermeulen, R. N. Schouten, C. Abellán *et al.*, Nature (London) **526**, 682 (2015).
[28] J. F. Clauser, M. A. Horne, A. Shimony, and R. A. Holt, Phys. Rev. Lett. **23**, 880 (1969).
[29] E. T. Campbell, M. J. Hoban, and J. Eisert, Quantum Inf. Comput. **14**, 0981 (2014).
[30] D. L. Deng and L. M. Duan, Phys. Rev. A **88**, 012323 (2013).
[31] D. J. Clarke, J. D. Sau, and S. Das Sarma, Phys. Rev. X **6**, 021005 (2016).
[32] J. Alicea, Y. Oreg, G. Refael, F. von Oppen, and M. P. A. Fisher, Nat. Phys. **7**, 412 (2011).
[33] B. S. Cirel'son, Lett. Math. Phys. **4**, 93 (1980).
[34] See Supplemental Material at http://link.aps.org/supplemental/10.1103/PhysRevLett.119.157702 for the calculation of the minimal entanglement and the detailed description of the measurement process.
[35] K. Flensberg, Phys. Rev. Lett. **106**, 090503 (2011).
[36] M. Leijnse and K. Flensberg, Phys. Rev. Lett. **107**, 210502 (2011).
[37] M. Field, C. G. Smith, M. Pepper, D. A. Ritchie, J. E. F. Frost, G. A. C. Jones, and D. G. Hasko, Phys. Rev. Lett. **70**, 1311 (1993).
[38] J. M. Elzerman, R. Hanson, J. S. Greidanus, L. H. Willems van Beveren, S. De Franceschi, L. M. K. Vandersypen, S. Tarucha, and L. P. Kouwenhoven, Phys. Rev. B **67**, 161308 (2003).
[39] J. M. Elzerman, R. Hanson, L. H. Willems van Beveren, B. Witkamp, L. M. K. Vandersypen, and L. P. Kouwenhoven, Nature (London) **430**, 431 (2004).
[40] J. R. Petta, A. C. Johnson, C. M. Marcus, M. P. Hanson, and A. C. Gossard, Phys. Rev. Lett. **93**, 186802 (2004).
[41] J. R. Petta, Science **309**, 2180 (2005).
[42] N. P. Oxtoby, H. M. Wiseman, and H.-B. Sun, Phys. Rev. B **74**, 045328 (2006).
[43] Z. Shi, C. B. Simmons, D. R. Ward, J. R. Prance, R. T. Mohr, T. S. Koh, J. K. Gamble, X. Wu, D. E. Savage, M. G. Lagally *et al.*, Phys. Rev. B **88**, 075416 (2013).
[44] D. R. Ward, D. Kim, D. E. Savage, M. G. Lagally, H. Foote, M. Friesen, S. N. Coppersmith, and M. A. Eriksson, npj Quantum Inf. **2**, 16032 (2016).
[45] Note that we do not demand a time-dependent control of the individual tunnel coupling matrix elements here, but rather an overall on-and-off switching of the QDs-Majorana coupling. The relative strength of the tunnel couplings $w_{j,k}$ can be fixed, e.g., at the fabrication stage.
[46] S. Popescu and D. Rohrlich, Phys. Lett. A **166**, 293 (1992).